Impacts of Numerical Weather Prediction Spatial Resolution On An Atmospheric Decision Aid For Directed Energy Weapon Systems

Randy J. Lefevre, Lt Col, USAF
Airborne Laser (ABL) Element Office
Kirtland AFB, NM

Frank H. Ruggiero
AFRL, Space Vehicles Directorate
Hanscom AFB, MA

Kevin P. Roe
Maui HPCC
Maui HI

Abstract

The Airborne Laser (ABL) is being developed as one element of our nation's Ballistic Missile Defense System. The ABL Element Office is developing an Atmospheric Decision Aid (ADA) to diagnose and forecast the location and magnitude of optical turbulence in the upper troposphere and lower stratosphere. Development of the ADA relies on an understanding about the strengths and weaknesses of numerical weather prediction (NWP) models, plus the sensitivity of the optical turbulence algorithms to the NWP spatial and temporal resolution. This case study compared the accuracy and precision of the ADA optical turbulence algorithms to several horizontal and vertical NWP resolutions. Results indicate that for a given vertical resolution using a finer horizontal resolution does not significantly improve the accuracy of the forecast, but for a given horizontal resolution increasing the vertical resolution does improve the forecast accuracy.

1. Introduction.

The Airborne Laser (ABL), an element of our nation's Ballistic Missile Defense System (BMDS), will detect and destroy boosting ballistic missiles. The ABL Element Office is managing the development of an Atmospheric Decision Aid (ADA) to diagnose and forecast the location and magnitude of optical turbulence in the upper troposphere and lower stratosphere. Optical turbulence is the fluctuation of density in the atmosphere and acts to defocus laser beams and thus reduce their effective range. Layers of intense optical turbulence, while possibly stretching hundreds of kilometers in the horizontal, tend to occur on vertical scales of a centimeter to 100 meters.

An objective method of predicting optical turbulence has been developed at the Air Force Research Laboratory (AFRL). This method combines the forecast output of numerical weather prediction (NWP) models with a parameterization of the optical turbulence tailored to the model (Ruggiero and DeBenedictis 2000, 2002). Others have also used this approach in support of astronomy operations (e.g. Businger et al. 2002). Ruggiero and DeBenedictis (2002) presented validation results that reveal the optical turbulence parameterization method is capable of representing coarse guidance on optical turbulence intensity. However the results also indicated that the predictive skill of the optical turbulence parameterization is limited by the ability of the NWP model to depict atmospheric features at a small spatial resolution.

The ABL's ADA is designed to use this objective optical turbulence prediction method. In practice the ADA will access real-time mesoscale NWP model forecast data from the Air Force Weather Agency

(AFWA). Given the ABL's need for small-scale vertical depiction of atmospheric phenomena and the operational constraints of the AFWA it is important to determine the optimal configuration in terms of grid spacing of the mesoscale model.

2. Problem and Methodology.

2.1 Mesoscale Forecast Model

The mesoscale model used in this study is the current operational model used at the AFWA—the Fifth Generation National Center for Atmospheric Research – Penn State University Mesoscale Model (MM5, version 3; Grell et al. 1995). This version of MM5 has been optimized for distributed memory, multiple processor computers such as the IBM SP series and scales efficiently (Michalakes, 2000). MM5 offers a selection of physics parameterizations and those used in this study were selected in order to mimic the MM5 setup used at the AFWA. Initial conditions and horizontal boundary conditions were obtained from the National Centers for Environmental Prediction's Global Forecast System (GFS).

2.2 Optical Turbulence Parameterization

The optical turbulence parameterization used in the ABL's ADA is taken from Dewan et al. (1993). It was developed using vertical wind profiles resolved on the order of meters and was originally designed to convert standard rawinsonde data into the refractive index structure function (C_n^2) profiles. The Dewan parameterization uses the Tatarski (1961) formulation for (C_n^2),

$$C_n^2 = 2.8\left(\frac{\left(79x10^{-6}P\right)}{T^2}\right)^2 L_o^{4/3}\left(\frac{\partial T}{\partial z}+\gamma\right)^2, \quad (1)$$

where P is the pressure in millibars, T is the temperature in degrees Kelvin, γ is the dry adiabatic lapse rate of $9.8x10^{-3}$ degrees Kelvin per meter and z is the height in meters. All of these variables are easily obtained from mesoscale NWP models, though it is not yet understood if the NWP models represent these variables at sufficient resolution. The one variable that can not be explicitly retrieved from a mesoscale model, $L_o^{4/3}$, is referred to by Tatarski (1961) as the outer length or the largest scale of the inertial subrange. Dewan et al. (1993) closed the Tatarski relationship for C_n^2 using a statistical relationships for $L_o^{4/3}$ developed as a function of wind shear. The relationships are:

$$L_o^{4/3} = 0.1^{4/3}\,x10^{(1.64+42.0xS)} \qquad \text{(Troposphere)}$$

$$(2)$$

$$L_o^{4/3} = 0.1^{4/3}\,x10^{(0.506+50.0xS)}, \qquad \text{(Stratosphere)}$$

where L_o has the units of meters and S is the magnitude of the wind shear,

$$S \equiv \left[\left(\frac{\partial u}{\partial z}\right)^2 + \left(\frac{\partial v}{\partial z}\right)^2\right]^{0.5}. \quad (3)$$

Ruggiero and DeBenedictis (2002) found the success of the Dewan model to diagnose optical turbulence is directly related to the ability of the mesoscale model to resolve the vertical wind shear (S).

2.3 Experiment Setup

In order to ascertain the optimal NWP model spatial configuration to predict optical turbulence, MM5 was run in triple nested form centered over the Mauna Kea Observatory on the island of Hawaii (Figure 1). The horizontal grid spacing for the three domains were 27, 9, and 3 kilometers, respectively. The 2-way feedback nest between grids was turned off in favor of one-way nesting where the outer grid provides the boundary conditions for next inner nest. This was done so that we could

Model Start Time (UTC)	Balloon #	Balloon Launch Time (UTC)
11 Dec 02 0600	001	12 Dec 02 0500
	002	12 Dec 02 0657
	003	12 Dec 02 0943
16 Dec 02 0600	007	17 Dec 02 0455
	008	17 Dec 02 0700
	009	17 Dec 02 0900

Table 1. MM5 model forecast start times and thermosonde balloon launch times used in study.

effectively judge the forecast skill of the coarser grids. MM5 was run in this horizontal configuration with 26 vertical levels used in one run and 52 vertical levels in the second run.

Validation for the optical turbulence predictions was carried out using C_n^2 observations collected by thermosondes during the Mauna Kea Fall 2002 measurement campaign. The principle of the thermosonde is described by Brown et al. (1982). The thermosonde makes precise simultaneous measurements of temperature using two probes separated by a horizontal distance of one meter. The theory of how C_n^2 is derived from the horizontal temperature difference in conjunction with the layer mean temperature and pressure is explained by Jumper and Beland (2000). The balloons carrying the thermosondes also carried a rawinsonde, which provided horizontal winds, temperature, moisture, and pressure measurements. All balloons were launched from Bradshaw Army Air Field, Hawaii located at 19° 47' N, 155° 33' W. During the experiment three balloons were launched approximately two hours apart on two different nights (Table 1). The MM5 model forecasts were started approximately 24 hours before the measurements commenced. This allowed the mesoscale model ample time to "spin up" small-scale features that would not be in the initial fields as well as simulate the forecast lead time that would be desired by ABL mission planners.

For each MM5 run the data from all three grids was output to a disk file every hour. After the model run was completed, C_n^2 was computed at each model grid point for each hour. A C_n^2 profile was then constructed along the balloon trajectory by spatial and temporal interpolation. Using the hypsometric equation, the C_n^2 values were interpolated vertically to 500 meter increments. The high-resolution thermosonde observations were binned into 500 meter layers and averaged to produce a layered mean C_n^2 value at same 500 meter vertical intervals.

3. Results.

We used two metrics to evaluate the impacts of spatial resolution on C_n^2. The accuracy of the forecasts was quantitatively assessed using root-mean-squared (rms) difference between the interpolated NWP forecasts and the thermosondes. The accuracy assessment was focused on the domain between 5 and 18 kilometers to be consistent with ABL operations. The accuracy results in Figure 2 show two trends. First that for a given vertical resolution, going to a finer horizontal resolution does not necessarily improve the accuracy; in fact the opposite appears to be true. However at a given horizontal resolution, increasing the number of vertical levels does appear to improve the accuracy of the C_n^2 predictions. In equations 1 and 2 it is obvious that C_n^2 is strongly dependent on the vertical shear of the horizontal wind and temperature. The rms differences between the model and observed horizontal winds and temperature are also plotted in Figure 2. Those results show that for temperature and wind, increasing the number of vertical levels from 26 to 52 at 27 and 9 kilometer horizontal grid spacing results in either improved or similar error. However at 3 kilometers, increasing the vertical levels appears to have a negative effect.

The second metric used to evaluate the impact of spatial resolution on C_n^2 was the precision of the forecasts. The precision of the forecasts is focused on identifying appropriate features in the vertical. As noted above, previous validation studies of mesoscale model-derived optical turbulence parameterizations have recognized that the mesoscale models do not produce atmospheric features at the resolution one would expect given the model grid spacing (Ruggiero and DeBenedictis 2002). Here we have computed the scaled power spectra for the vertical profiles corresponding to the thermosonde flight paths of the east-west component of the wind (u), and the north-south component (v), plus the temperature. The power spectra for temperature and the v-component wind are given in Figure 3. For temperature there is a substantial difference between the 26 and 52 level forecasts. The 26 level forecasts tend to have most power in the longer wavelengths, regardless of the horizontal resolution. At the shorter wavelengths, particularly near three kilometers, there is significant deviation from the observed spectra. The 52 level forecasts tend to follow the observed spectra closer, but still shows a substantial deviation from it. The v-component of the observed profile has similar spectra to that of temperature, including the peak at approximately three kilometers. The model runs behave a little differently here, in that two closest model runs to capturing this secondary peak are 26 level runs.

4. Significance to DoD.

This work will determine what is the best mesoscale model spatial resolution, both in the vertical and horizontal, for predicting optical turbulence with the Dewan et al. model (1993). It will aid in the eventual operations of the Airborne Laser. Being able to know the potential atmospheric effects on the lasers' propagation will allow mission planners to optimally locate the ABL's orbit to protect the asset while maximizing the lethality capability.

5. Systems Used

All NWP forecasts using the MM5 model and optical turbulence postprocessor were run on the Maui High Performance Computing Center IBM P690. Portions of these computations were carried out under the High Performance Modernization Office's Airborne Laser II Challenge project. Part of the data analysis work was performed on the Aeronautical Systems Center IBM P3.

6. CTA.

This work falls under the Climate/Weather/Ocean (CWO) arena.

7. References.

Brown, J, H., R. E. Good, P.M. Bench, and G. Faucher, 1982: Sonde measurement for comparitive measurements of optical turbulence. Air Force Geophysics Laboratory Technical Report, AFGL-TR-82-0079. ADA 118740

Businger, S., R. McLaren, R. Ogasawara, D. Simons, and R. J. Wainscoat, 2002: Starcasting. *Bull. Amer. Meteor. Soc.,* **83**, 858-871.

Dewan, E. M., R. E. Good, B. Beland, and J. Brown, 1993*: A Model for C_n^2 (Optical Turbulence) Profiles using Radiosonde*

Data. Phillips Laboratory Technical Report, PL-TR-93-2043. ADA 279399.

Grell, G. A., J. Duhia, and D. R. Stauffer, 1995: *A description of the fifth generation Penn State/NCAR Mesoscale Model (MM5).* NCAR Tech. Note T/N-398 + STR, 122 pp. [Available from NCAR Information Services, P.O. Box 3000, Boulder, CO 80307] (http://www.mmm.ucar.edu/mm5/documents/mm5-desc-doc.html)

Jumper, G. Y., and R. R. Beland, 2000: Progress in the understanding and modeling of atmospheric optical turbulence. 31st AIAA Plasma Dynamics and Laser Conf., 19-22 June 2000, Denver, Co.

Michalakes, J., 2000: The same-source parallel MM5. *Sci. Programming*, **8**, 5-12. (http://www.mcs.anl.gov/~michalakes/JOSP-michalakes.ps)

Ruggiero, F. H. and D. A DeBenedictis, 2002: Forecasting Optical Turbulence from Mesoscale Numerical Weather Prediction Models. Preprints, *2002 DoD High Performance Modernization Program Users Group Conference*, 10-14 Austin TX. (http://www.hpcmo.hpc.mil/Htdocs/UGC/UGC02/paper/frank_ruggiero1_paper.pdf)

Ruggiero, F. H., and D. A. DeBenedictis, 2000: Three-Dimensional Modeling of Optical Turbulence. Preprints, *2000 DoD High Performance Modernization Program Users Group Conference*, 5-8 June, Albuquerque NM. (http://www.hpcmo.hpc.mil/Htdocs/UGC/UGC00/paper/frank_ruggiero_paper.pdf)

Tatarski, V. I., 1961: Wave Propagation in a Turbulent Medium, McGraw-Hill.

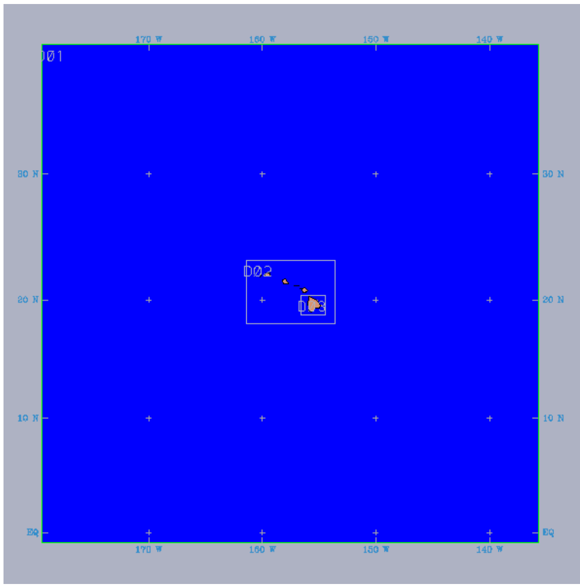

Figure 1. Depiction of three horizontal nests used in this study.

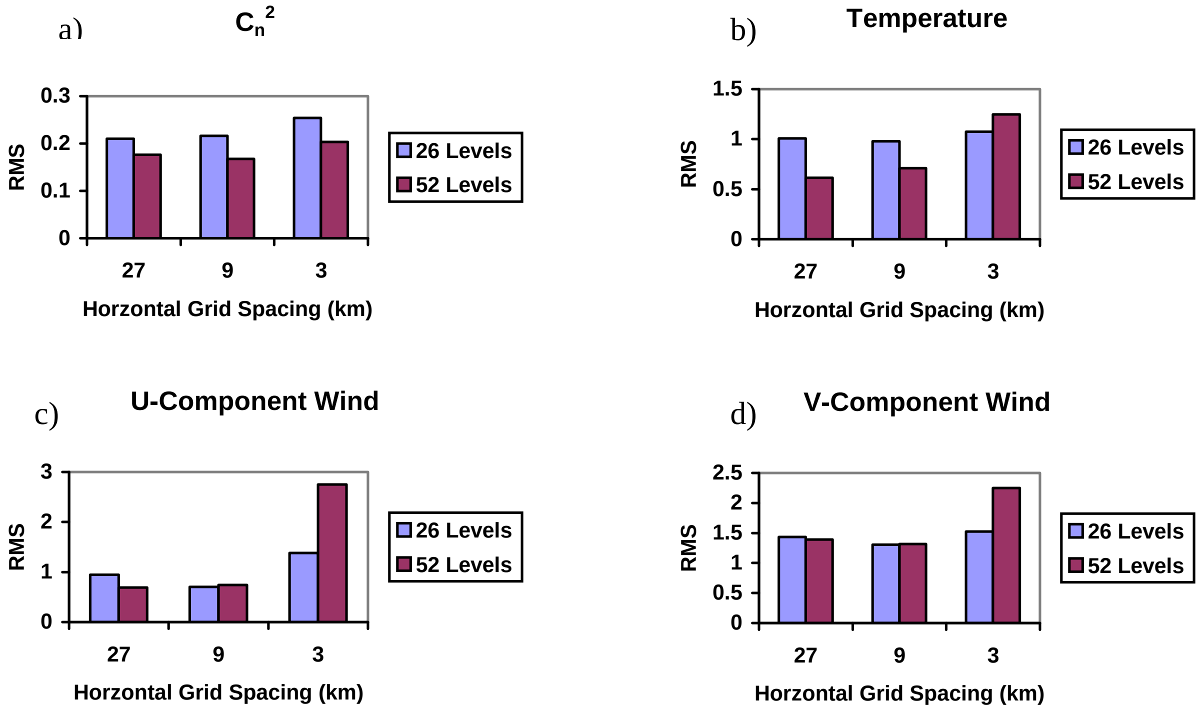

Figure 2. Root-mean-squared difference of a) C_n^2, b) temperature, c) u-component of the horizontal wind, and d) v-component of the horizontal wind between model runs at varying horizontal and vertical resolutions and observed values for the heights of 5 to 18 km MSL along thermonsonde flight paths.

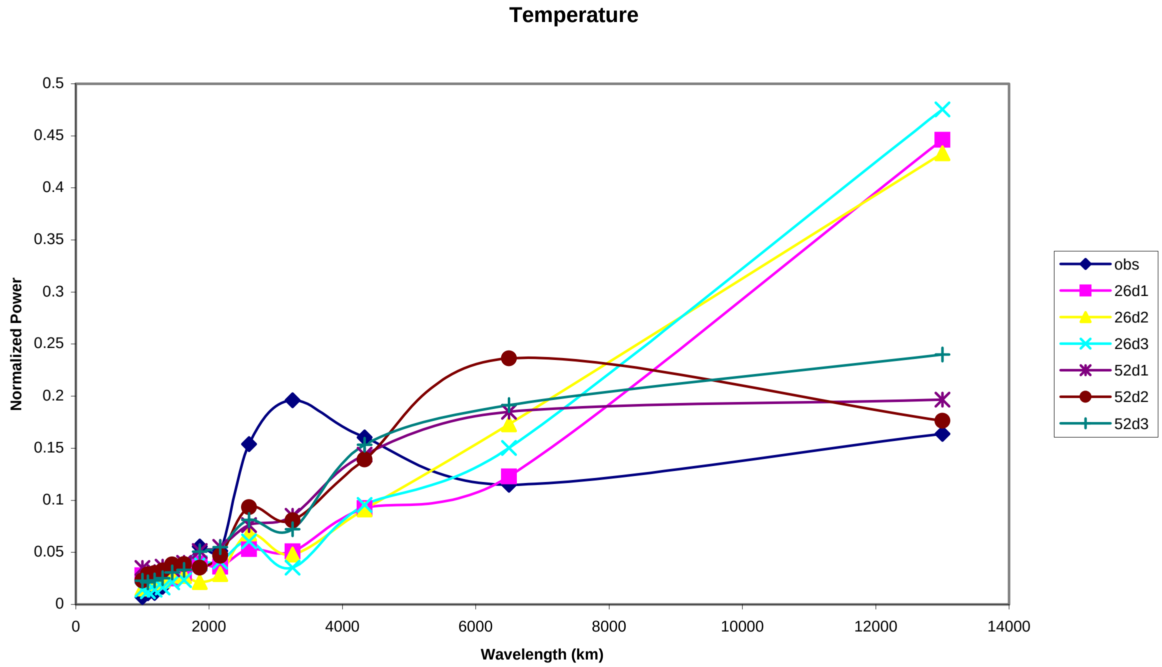

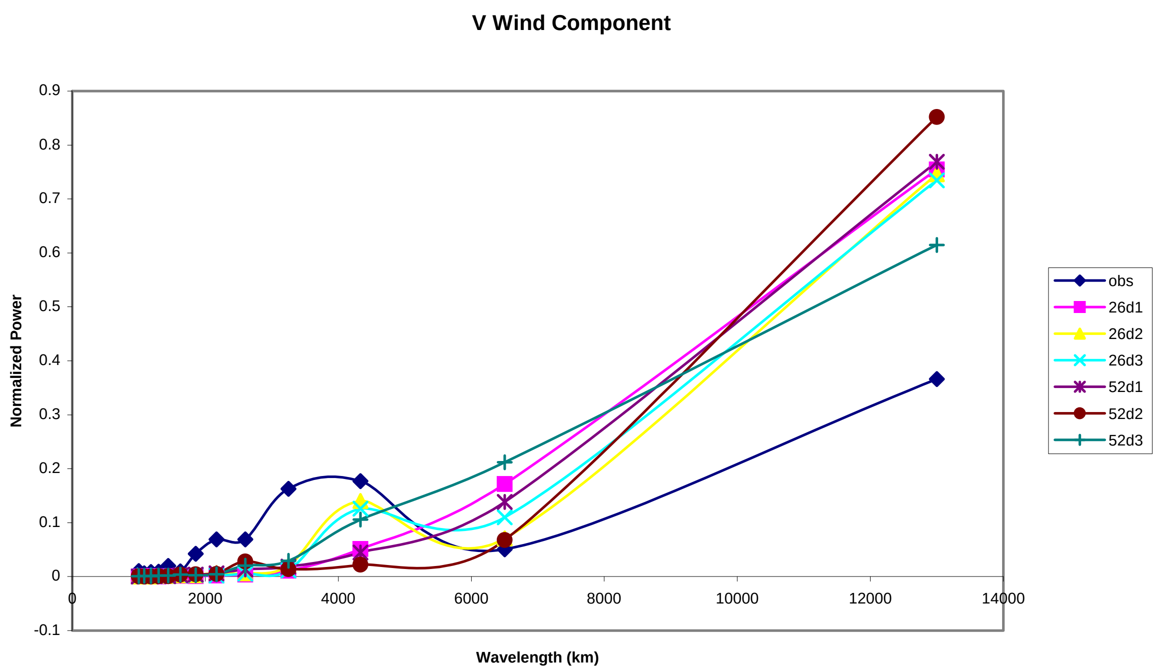

Figure 3. Average power spectra plots for temperature and v-component horizontal wind for the observed profiles and the six different model resolution configurations.